NEURAL REGENERATION RESEARCH
Volume 7, Issue 16, June 2012
www.nrronline.org

Cite this article as: Neural Regen Res. 2012;7(16):1205-1212.

Autophagy and apoptosis during adult adipose-derived stromal cells differentiation into neuron-like cells *in vitro*★

Yanhui Lu[1], Xiaodong Yuan[1], Ya Ou[1], Yanan Cai[1], Shujuan Wang[1], Qiaoyu Sun[1], Wenli Zhang[2]

1*Department of Neurology, Kailuan General Hospital, Hebei Union University, Tangshan 063000, Hebei Province, China*
2*Hebei Union University, Tangshan 063000, Hebei Province, China*

Abstract

β-mercaptoethanol can induce adult adipose-derived stromal cells to rapidly and efficiently differentiate into typical neuron-like cells *in vitro*. Immunohistochemistry showed that neuron specific enolase and neurofilament-200 expression gradually increased with the extension of induction time, and peaked at 5 hours. By contrast, glial fibrillary acidic protein was negatively expressed at all time points. Induced cells possessed a typical Nissl body, apoptosis showing condensed chromatin in the nucleus, autophagosomes with a bilayered membrane and autolysosomes in the cytoplasm at 5 hours. TUNEL assay and immunohistochemistry and immunofluorescence demonstrated that apoptosis and caspase-3 expression increased and peaked at 8 hours. Immunohistochemistry and immunofluorescence showed that microtubule-associated protein light chain 3 gradually increased with induction and reached a peak at 5 hours. These results indicate that autophagy played an important role in protecting cells during adult adipose-derived stromal cells differentiation into neuron-like cells *in vitro*.

Key Words

adult adipose-derived stromal cells; neuron-like cells; differentiation; apoptosis; autophagy; neural regeneration

Abbreviations

ADSCs, adipose-derived stromal cells; NSE, neuron specific enolase; NF-200, neurofilament-200; GFAP, glial fibrillary acidic protein

Yanhui Lu★, Studying for master's degree, Department of Neurology, Kailuan General Hospital, Hebei Union University, Tangshan 063000, Hebei Province, China

Corresponding author: Xiaodong Yuan, Professor, Chief physician, Master's supervisor, Department of Neurology, Kailuan General Hospital, Hebei Union University, Tangshan 063000, Hebei Province, China
yxd68@sohu.com

Received: 2012-02-20
Accepted: 2012-05-03
(N20111126002/YJ)

Lu YH, Yuan XD, Ou Y, Cai YN, Wang SJ, Sun QY, Zhang WL. Autophagy and apoptosis during adult adipose-derived stromal cells differentiation into neuron-like cells in vitro. Neural Regen Res. 2012;7(16):1205-1212.

www.crter.cn
www.nrronline.org

doi:10.3969/j.issn.1673-5374.2012.16.001

INTRODUCTION

Adult adipose-derived stromal cells (ADSCs) can differentiate into neuron-like cells *in vitro* in the presence of inducers, as this cell type crosses germ layers and has the ability to differentiate into multiple cell types[1-5]. Using ADSCs in experimental studies has many advantages, and therefore these cells have become one of the most used stem cells in transplantation studies for the treatment of central nervous system disorders. However, ADSC-derived neurons usually have a short survival, even dying a few hours after induction and differentiation[6-7]. This observation means that it is impossible for these cells to proliferate effectively. It is not clear, however, why this short survival time occurs[5-6, 8]. Apoptosis and autophagy play an important role in cell death. Autophagy allows the intracellular management and control of proteins and organelles within the cells. This process occurs when cells degrade impaired organelles and macromolecules by lysosomes[7]. A previous study has confirmed that apoptosis was present in the differentiation process of ADSCs[9]. The role of autophagy as a programmed cell death is not clear. This study, therefore, sought to

examine apoptosis and autophagy-related features during ADSC differentiation into neuron-like cells following exposure to β-mercaptoethanol *in vitro* to analyze the mechanisms leading to the death of neuron-like cells.

RESULTS

Morphological changes in adult ADSCs before and after induction

Newly extracted primary adult ADSCs were suspended in culture medium. The cells adhered within 24 hours and appeared as circular shapes under inverted phase contrast microscopy (Figure 1A). At 3–6 passages, cells were purified with cell shape becoming uniform and exhibiting a fibroblast-like morphology and swirl-like growth (Figures 1B, C). After induction, the cytoplasm retracted toward the nucleus, the nuclei became round and enlarged, and clear halos were visible around the cell body (Figures 1D–F). Following 5 hours of induction, cells exhibited a typical neuronal morphology, *i.e.*, a small conical cell body retracted toward the nucleus. Cell body refraction was obviously enhanced, and long axon-like processes with branched endings were also observed (Figure 1G). The morphology of differentiated cells did not change significantly at 8 hours (Figure 1H). After 8 hours, the cells gradually died, and many cells separated from the culture bottle. Most cells had died after 12 hours.

Neuron specific enolase (NSE), neurofilament-200 (NF-200) and glial fibrillary acidic protein (GFAP) expression in induced adult ADSCs

NSE and NF-200 were not expressed in adult ADSCs before induction. Both proteins were expressed in the pre-induction, and induction groups at 1, 3, 5, and 8 hours. Staining was seen as brown cytoplasm and increased gradually over time. Expression of both markers reached a peak at 5 hours after induction ($P < 0.05$). No significant difference in the expression of NSE and NF-200 protein was observed between the induction groups at 5 and 8 hours ($P > 0.05$). The expression of GFAP was negative in the non-induction, pre-induction, and induction groups at 1, 3, 5, and 8 hours (Table 1, Figures 2, 3).

Caspase-3, light chain 3 and TUNEL expression in adult ADSCs after induction

Caspase-3 and light chain 3 expression was seen in the cytoplasm, and was greater in the cell body than cell processes. Caspase-3 and light chain 3 expression was determined in nuclei at 5 and 8 hours after induction. ADSCs displayed red fluorescence (Figure 3). Light chain 3 expression was detected in the pre-induction group and peaked at 5 hours after induction. There were significant differences between each time point except in the 5 and 8 hour induction groups (Table 1, Figure 3).

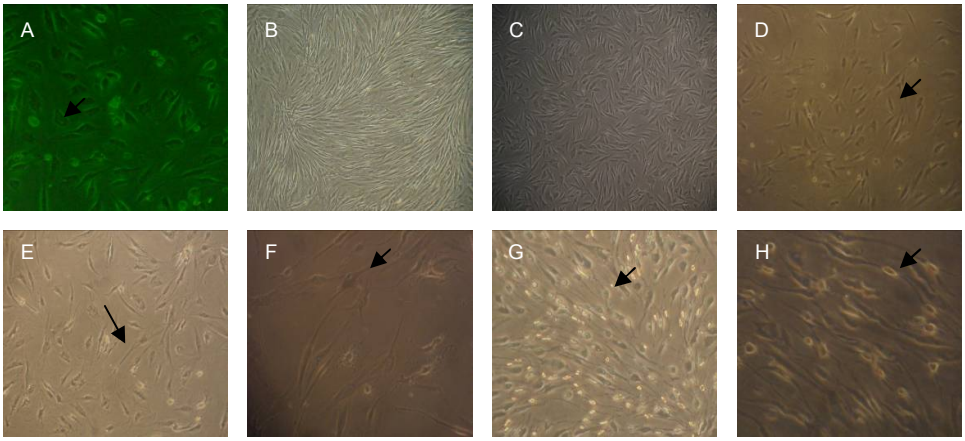

Figure 1 Morphological changes in adult adipose-derived stromal cells before and after induction (inverted contrast microscopy, × 100).

(A) Primary culture at 24 hours, the arrow indicates a short spindle cell.

(B) Cells at passage 3 and cultured for 10 days displayed swirl-like growth.

(C) Cells at passage 4 and cultured for 1 day adhered and exhibited fibroblast-like shape.

(D) Cells pre-induced for 24 hours, the arrow indicates enhanced cell body refraction.

(E) Cells induced for 1 hour, the arrow indicates axon-like processes.

(F) Cells induced for 3 hours, the arrow indicates neuron-like cells.

(G, H) Cells induced for 5 and 8 hours exhibited the typical morphology of neurons. The arrow indicates axon- and dendrite-like structures.

Table 1 Changes in percentage positive cells of neurofilament-200 (NF-200), neuron specific enolase (NSE), glial fibrillary acidic protein (GFAP), caspase-3, light chain 3 (LC3) and TUNEL (%)

Group	NF-200	NSE	GFAP	Caspase-3	LC3	TUNEL
Preinduction	4.80±2.17	1.49±1.46	0	0	2.24±2.13	0
Induction for 1 hour	33.17±1.24	42.97±1.41	0	1.71±2.15	31.98±1.71[a]	1.39±0.34
Induction for 3 hours	57.32±1.92	62.73±0.52	0	13.47±3.67	51.65±8.81	6.23±0.32
Induction for 5 hours	78.76±0.57[a]	84.20±1.22[a]	0	23.23±2.59	77.29±3.93	20.67±0.78
Induction for 8 hours	77.64±1.11	83.73±0.51	0	32.44±2.80	68.28±1.74	28.34±0.62

Data are expressed as mean ± SD. Differences between multiple groups were tested using one-way analysis of variance, and intergroup differences were compared using Student-Newman-Keuls test. [a]$P < 0.05$ *vs.* induction for 1, 3 and 5 hours groups.

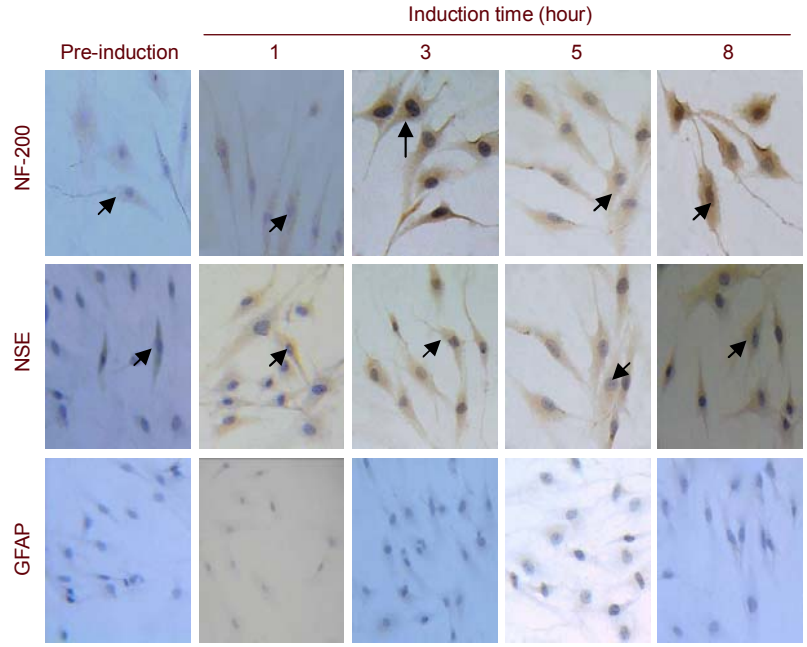

Figure 2 Neurofilament-200 (NF-200), neuron specific enolase (NSE) and glial fibrillary acidic protein (GFAP) expression in adult adipose-derived stromal cells after induction (light microscope, × 100).

The arrows indicate positive NF-200 and NSE expression. The expression of NF-200 increased gradually in the cytoplasm over time and peaked at 5 hours.

The expression of NSE increased gradually in the cytoplasm with time and also peaked at 5 hours. GFAP expression was negative.

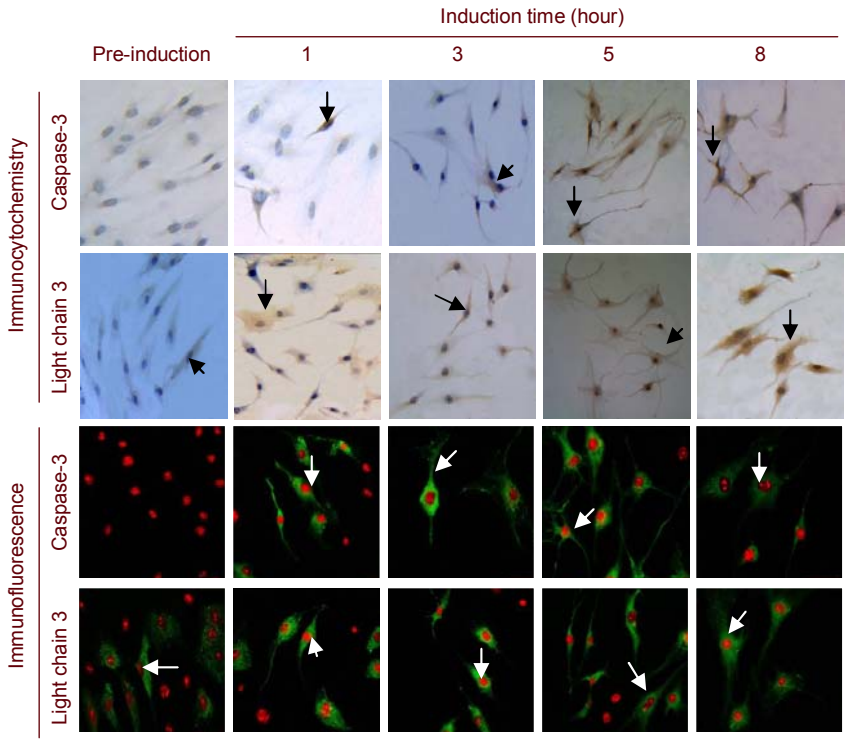

Figure 3 Caspase-3 and light chain 3 expression in induced adult adipose-derived stromal cells (light microscope, × 100).

The expression of caspase-3 and light chain 3, seen using immunocytochemistry, in the pre-induction, and induction groups at 1, 3, 5, and 8 hours.

The arrows indicate positive cells with brown cytoplasm and blue nucleus.

The expression of caspase-3 and light chain 3 were seen using immunofluorescence in all groups.

The arrows indicate positive cells with green fluorescing cytoplasm and red fluorescent nuclei (laser confocal microscope, × 400). Fluorescein isothiocyanate was used.

Both caspase-3 and TUNEL analyses revealed negative expression in the pre-induction group. Positive expression appeared in cells after induction for 1, 3, 5 and 8 hours. Positive staining increased with prolonged time and reached a peak at 5 hours after induction ($P < 0.05$). TUNEL analysis revealed that after induction for 1, 3, 5 and 8 hours, neuron-like cells exhibited nuclear condensation and accumulation of dense and dyed brown particles around the inner surface of the nuclear membrane (Figure 4). Different test indicators in the same group were compared and revealed that staining for NSE and light chain 3 was not significantly different to the pre-induction group ($P > 0.05$). No significant difference between NF-200 and light chain 3 was observed at 1, 3 and 5 hours after induction ($P > 0.05$). Significant differences were detectable in NF-200, NSE and light chain 3 expression at 8 hours post-induction ($P < 0.05$). Caspase-3 and TUNEL labeling was similar at 1 and 8 hours post-induction ($P > 0.05$; Table 1, Figures 3, 4).

Ultrastructure of ADSC-derived neuron-like cells (Figure 5)

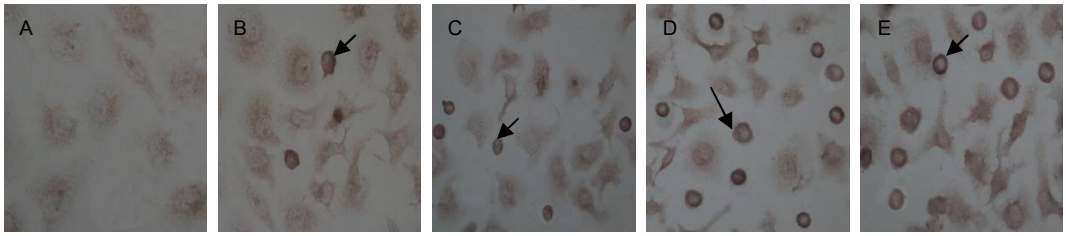

Figure 4 Apoptosis of adipose-derived stromal cell-derived neuron-like cells (TUNEL staining, light microscope, × 100).

(A) There were no apoptotic cells following pre-induction.

(B–E) Apoptotic cells were seen at 1, 3, 5 and 8 hours after induction. Arrows indicate nuclei of positive cells.

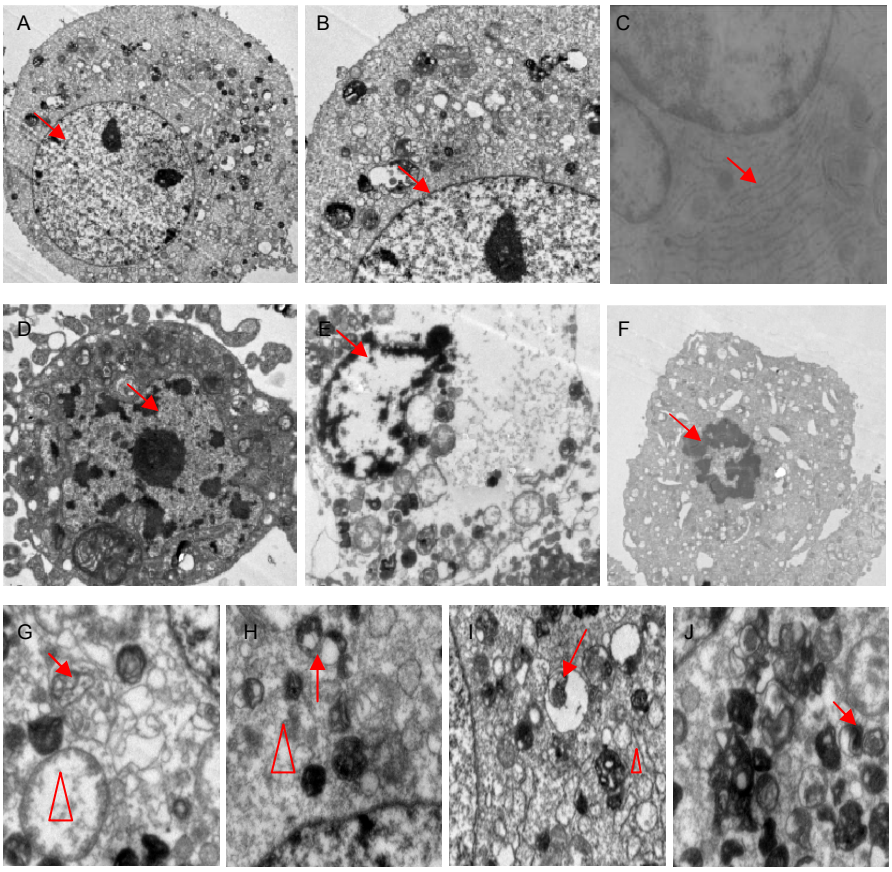

Figure 5 Ultrastructure of normal adipose-derived stromal cell-derived neuron-like cells after 5 hours of induction under transmission electron microscopy.

(A) The arrow indicates a large round nucleus with a large amount of euchromatin, but little heterochromatin (× 5 000).

(B) A large number of cytoplasmic organelles. The arrow indicates the mitochondria (× 8 000).

(C) The arrow indicates a large number of Nissl bodies (× 10 000).

(D–F) Apoptotic neuron-like cells at different stages of apoptosis. The cell body of some neuron-like cells was reduced in size, nuclei were irregular, and chromatin was split into fragments (D, × 10 000). Chromatin was highly condensed and scattered to the periphery. The nuclear membrane was still intact (E, × 10 000). Nuclear membrane disappeared and chromatin split into fragments (F, × 1 000). The arrows indicate broken chromatin.

(G–J) Autophagic cells (× 10 000). (G) The arrow indicates an autophagy with swallowed mitochondria. (H–J) Autolysosomes are indicated. (H) The triangle indicates normal lysosomes. (I) The triangle indicates outstretched endoplasmic reticulum. The triangle indicates swelling of mitochondria.

At 5 hours after induction, the ultrastructure of normal ADSC-derived neuron-like cells was observed using transmission electron microscopy. Our results revealed that cells were generally round and that the cell surface was not smooth, but had many processes. A large round nucleus was present, as was a lightly-stained double-layered membrane, and a large amount of euchromatin, but little heterochromatin. There were a large number of cytoplasmic organelles including mitochondria, endoplasmic reticulum, Golgi complex structures, and a large number of Nissl bodies (Figures 5A–C). Reduced cell body size of some neuron-like cells, less processes, irregular nuclei, retracted nuclear membranes, and some vanished nucleolus were observed. Euchromatin was scarce, but heterochromatin was common. This chromatin was highly condensed and scattered in the periphery, and even the nuclei were split into fragments. In addition, cytoplasmic organelles were abundant. Some mitochondria appeared edematous, showing increased volume, cristae rupture and vacuolar degeneration (Figures 5D–F). In addition, the cytoplasm of some neuron-like cells had a large number of outstretched endoplasmic reticuli and “C”-shaped double-membrane autophagosomes also appeared. The autophagosome contained engulfed mitochondria and an autolysosome emerged from the autophagosome. Primary lysosomes contained dense phagocytic particles (Figures 5G–J).

DISCUSSION

The reasons for the death of ADSC-derived neuron-like cells during the induction process have not been extensively studied. Apoptosis was thought to be a main cause of cell death[9], but the role of autophagy is not clear. A previous study has shown that cell autophagy occurred once stimuli was applied or in the presence of a change to external conditions[7]. This autophagy had a protective effect on cells by removing damaged organelles and restricting the release of apoptotic factors into the cytoplasm. However, excessive, insufficient autophagy or incomplete autophagy may cause and accelerate cell death[7, 10-13]. Adult ADSCs differentiated into neuron-like cells with inducer medium containing a small dose of β-mercaptoethanol in the pre-induction group. Induced cells expressed NSE and NF-200, which are cytoplasmic protein markers for neurons[14]. Non-induced adult ADSCs do not express NSE[5]. This evidence illustrates that ADSCs differentiate into neuron-like cells during pre-induction. Meanwhile, our results showed that the expression of light chain 3, the most reliable marker of an autophagosome membrane, was positive in the pre-induction group[15]. By contrast, caspase-3, the main initiator of apoptosis, was not detected by immunocytochemistry or immunofluorescence in this group. Furthermore, apoptotic cells were not detected using TUNEL, a technique to detect apoptosis at the single cell level[16]. All these findings suggested that cell autophagy was activated by adult ADSC differentiation using low-dose β-mercaptoethanol as an inducer and no positive apoptotic cells existed in the pre-induction stage. Therefore, autophagy played an important role in cell growth and differentiation, removing useless and damaged organelles and macromolecules and protecting cells from apoptosis or death.

With a large dose of β-mercaptoethanol inducer, we found cell body contraction, neurite elongation and apparent change in phenotype using inverted contrast microscopy. Immunohistochemistry and immunofluorescence revealed that the expression of light chain 3 increased with prolonged induction time and reached a peak at 5 hours after induction. Autophagy and cell differentiation rate were similar, but were higher than the apoptosis rate in the pre-induction group, and induction groups at 1 and 3 hours. Transmission electron microscopy revealed ultrastructural features of autophagy which included a large number of outstretched endoplasmic reticula, swollen mitochondria, autophagosomes with swallowed mitochondria and autolysosomes containing dense phagocytic particles. Apoptosis, however, has been reported to be initiated by autophagy[13, 17-18]. Studies had shown that caspase-3, which is a key element involved in apoptotic signaling, was activated in the early stage of apoptosis, and existed in the cytoplasm[19-20]. Gavrieli *et al* [21-22] in 1992 proposed that the TUNEL assay, at the single cell level, detected apoptotic nuclei or apoptotic bodies of apoptotic cells. This method was thought to be specific, highly sensitive, qualitative, quantitative and allowed multi-parameter detection of apoptotic cells. Our results showed that positive expression of caspase-3 existed mainly in the cytoplasm. TUNEL analysis revealed that neuron-like cells, after induction for 1 hour, exhibited nuclear condensation and a nuclear membrane around the inner surface of the nucleus. Accumulation of dense and dyed brown particles was also observed in this area. The amount of particles increased gradually over time, which indicated that apoptosis of ADSC-derived neuron-like cells was obviously correlated with an induced reaction. Some neuron-like cells appeared to demonstrate ultrastructural features of apoptosis, showing reduced cell body size, irregular nuclei, retracted nuclear membranes, aggregated and marginated chromatin, nuclei split into fragments, concentrated cytoplasmic organelles, edematous mitochondria and vacuolar degeneration 5 hours after induction.

Approximately 28% of cells were apoptotic 8 hours after induction. Caspase-3 was detected as a core protease in 32.44% of cells, which suggested that the apoptotic response would not stop at this time point but would continue to rise. A large number of cells had died at 8 hours. A previous study has also shown that the number of viable cells decreased over time[9]. Thus, a formal inducer can not only stimulate cell-surface channels or receptors to change cell phenotype and morphology, but also initiate apoptosis secondary to autophagy. The percentage of apoptosis rose with prolonged induction time, indicating that apoptosis is one important cause of adult ADSC-derived neuron-like cell death.

A previous study demonstrated that the total number of cells in the 1 hour induction group was significantly lower than that in pre-induction group. Cell number was stable in the 1, 3 and 5 hour induction groups and was significantly reduced at 8 hours[7]. In our study, autophagy and apoptosis appeared in numerous cells at the start of formal induction. The incidence rate of the two mechanisms increased gradually with prolonged induction time. The peak percentage of autophagy at 5 hours was similar to that at 8 hours, but apoptosis was still continuing to rise. In fact, the deaths of many cells were observed using microscopy. This result suggested that autophagy, activated by external stimuli, played an important role in protecting cells and also induced apoptosis during adult ADSC differentiation into neuron-like cells. However, autophagy at 8 hours was not satisfied with the needs of cell growth and differentiation and activated the apoptosis program to cause or accelerate apoptosis through releasing apoptotic factors from the collapse of damaged mitochondria, as has been shown in previous studies[23-26]. Our results revealed that both caspase-3 and light chain 3 were expressed mainly in the cytoplasm. The majority of expression was distributed in cell bodies around the nucleus and was weak in cell processes. Autophagosomes eliminated the damaged mitochondria during cell growth and differentiation. Thus, this study found that autophagy occurred earlier and more often in the cell body to remove the damaged mitochondria during cell growth and differentiation, preventing caspase-3 and other key factors from release and activation thereby avoiding starting apoptosis. In addition, the nuclei of cells with autophagy displayed the integral outline and normal red fluorescence appeared only in a few spots of the nucleus, which were similar to the apoptotic nuclei. The result confirmed that autophagy accompanied apoptosis. The coexistence of apoptosis and autophagy prompted us to continue further studies into a method to protect cells and inhibit cell death effectively, thereby prolonging the survival time of the target cells.

In summary, caspase-dependent apoptosis is one of the most important reasons leading to cell death during adult ADSC differentiation into neuron-like cells. Autophagy plays an important role in cell protection, and cell growth, maturation and death regulation. Autophagic insufficiency or damage is a significant reason for causing or accelerating apoptosis.

MATERIALS AND METHODS

Design

Cytological *in vitro* experiment.

Time and setting

Experiments were performed at the Central Laboratory of Hebei Union University, China, from March 2010 to November 2011.

Materials

A total of 10–60 mL abdominal, subcutaneous, fatty tissue was obtained, using the needle method, from healthy adult volunteers undergoing liposuction. Volunteers were aged 20–35 years and tissue collection occurred at the Cosmetology Department, Kailuan General Hospital affiliated to Hebei Union University, China. Protocols were conducted in accordance with the *Administrative Regulations of Medical Institutions*, State Council of China[27], and written informed consent was obtained.

Methods

Extraction and culture of adult ADSCs

Adult ADSCs were isolated and cultured from adipose tissue of healthy volunteers according to the method by Ye *et al* [5]. Isolated ADSCs were cultured in a 5% CO_2 humidified incubator at 37°C. The medium was then replaced every 2–3 days. Confluence was observed at 10–14 days, and cells were passaged at a ratio of 1:2[28-29].

Induction and differentiation of adult ADSCs into neuron-like cells in vitro

Passages 3–6 adult ADSCs were digested and seeded onto culture plates. Cells were maintained in preinduction medium containing 1 mM β-mercaptoethanol (Sigma, St. Louis, MO, USA), 20% fetal calf serum and high glucose-Dulbecco's modified Eagle's medium (DMEM; Hyclone, Logan, Utah, USA) for 24 hours until reaching 70–80% confluency, whereupon the cells were placed in formal induction medium (5 mM β-mercaptoethanol, DMEM). Cells were assigned to pre-induction, 1, 3, 5, and 8 hour induction groups[30-32]. The cell morphology of each group was

observed under inverted phase contrast microscopy (Nikon, Tokyo, Japan).

NF-200, NSE, GFAP, Caspase-3 and light chain 3 expression, as detected by immunocytochemistry and immunofluorescence

Cells were fixed with 4% paraformaldehyde for 30 minutes, treated with 0.1% Triton-X 100 for 8 minutes, and incubated with 3% H_2O_2 for 10 minutes to eliminate endogenous peroxidase. Cells were then incubated in working solutions of primary antibodies: rabbit anti-human NSE, NF-200, GFAP, light chain 3 (1:100; Beijing Biosynthesis Biotechnology, Beijing, China) and rabbit anti-human caspase-3 (1:100; Wuhan Boster, Wuhan, China) at 4°C overnight. For immunocytochemistry, goat anti-rabbit IgG antibody-horseradish peroxidase polymer (ready to use, Beijing Zhongshan Gold Bridge, Beijing, China) was added for 15 minutes at room temperature. A diaminobenzidine kit (Beijing Zhongshan Gold Bridge) was used to label the antibodies for 10 minutes, and the reaction was terminated with tap water. Cells were counterstained with hematoxylin, dehydrated with gradient alcohol, followed by xylene. Finally, the stained cells were photographed utilizing an optical microscope (Nikon). The percentage of positive cells in 100-fold fields was calculated. Each field was quantified three times, and an average value was obtained from five fields. For immunofluorescent staining, a fluorescein isothiocyanate-labeled goat anti-rabbit IgG antibody-horseradish peroxidase polymer (1:200; Beijing Zhongshan Gold Bridge) was used, followed by propidium iodide counterstaining. Cells were observed and photographed under a laser confocal microscope (Olympus, Tokyo, Japan) to evaluate caspase-3 and light chain 3 expression.

Assessment of apoptosis in ADSC-derived neuron-like cells using TUNEL staining

Cells were fixed after pre-induction and induction for 1, 3, 5, 8 hours. To each coverslip, 20 μL buffer, 1 μL TdT, 1 μL DIG-d-UTP, and 18 μL labeling buffer (Roche, Nutley, NJ, USA) was added. Cells were incubated for 2 hours at 37°C, and then blocking reagent (50 μL/cover slip) was added at room temperature for 30 minutes. Cells were then incubated with biotinylated digoxin antibody 50 μL/cover slip (Roche) at 37°C for 30 minutes, and washed four times in PBS. Expression was then observed using diaminobenzidine coloration. Cells were observed and recorded under an optical microscope (JNOEC, Nanjing, China). The percentage of TUNEL-positive cells from each group was quantified under a high power field (100 ×). Each field was quantified three times, and an average value was obtained from five fields.

Ultrastructure, apoptosis and autophagy of ADSCs after induction, as observed by transmission electron microscope

Cells induced for 5 hours were digested, centrifuged, and fixed in 3% glutaraldehyde and 1% osmic acid, followed by propionaldehyde dehydration, and epoxy resin embedding. Cells were sliced using a thin slicing machine and stained using 2% uranyl acetate and lead citrate. Images were observed and recorded using transmission electron microscopy (Hitachi, Tokyo, Japan).

Statistical analysis

All experimental data were analyzed using Microsoft Excel 2003 (Microsoft, Washington, USA) and SPSS 13.0 (SPSS, Chicago, IL, USA). Measurement data were expressed as mean ± SD. Multiple group differences were compared using one-way analysis of variance, while intergroup differences were compared using Student-Newman-Keuls test only. A value of $P < 0.05$ was considered statistically significant.

Acknowledgments: We appreciate the assistance given by staff from the Department of Immunocytochemistry concerning experimental techniques and equipment. We also extended out gratitude to the Neurology Laboratory of Kailuan General Hospital, Hebei Union University, China.

Author contributions: Yanhui Lu was responsible for writing the manuscript, study design, implementation, and data arrangement. Xiaodong Yuan was responsible for the study design, organization, result analysis and manuscript authorization. Ya Ou, Yanan Cai and Qiaoyu Sun participated in the study design, and performed experiments. Shujuan Wang and Wenli Zhang performed data collection and integration.

Conflicts of interest: None declared.

Ethical approval: This study was approved by the Ethics Committee of Kailuan General Hospital, China.

REFERENCES

[1] Zuk PA, Zhu M, Ashjian P, et al. Human adipose tissue is a source of multipotent stem cells. Mol Biol Cell. 2002; 13(12):4279-4295.

[2] Guilak F, Lott KE, Awad HA, et al. Clonal analysis of the differentiation potential of human adipose-derived adult stem cells. J Cell Physiol. 2006;206(1):229-237.

[3] Ning H, Lin G, Lue TF, et al. Neuron-like differentiation of adipose tissue-derived stromal cells and vascular smooth muscle cells. Differentiation. 2006;74(9-10):510-518.

[4] Ning H, Lin G, Fandel T, et al. Insulin growth factor signaling mediates neuron-like differentiation of adipose-tissue-derived stem cells. Differentiation. 2008;76(5): 488-494.

[5] Ye CQ, Yuan XD, Liu H, et al. Ultrastructure of neuronal-like cells differentiated from adult adipose-derived stromal cells. Neural Regen Res. 2010;5(19): 1456-1463.
[6] Safford KM, Safford SD, Gimble JM, et al. Characterization of neuronal/glial differentiation of murine adipose-derived adult stromal cells. Exp Neurol. 2004; 187(2):319-328.
[7] Eskelinen EL, Saftig P. Autophagy: a lysosomal degradation pathway with a central role in health and disease. Biochim Biophys Acta. 2009;1793(4):664-673.
[8] Ou Y, Yuan XD, Cai YN, et al. Ultrastructure and electrophysiology of astrocytes differentiated from adult adipose-derived stromal cells. Chin Med J (Engl). 2011; 124(17):2656-2660.
[9] Cai YN, Yuan XD, Ou Y, et al. Apoptosis during β-mercaptoethanol-induced differentiation of adult adipose-derived stromal cells into neurons. Neural Regen Res. 2011;6(10):750-755.
[10] Oh SY, Choi SJ, Kim KH, et al. Autophagy-related proteins, LC3 and Beclin-1, in placentas from pregnancies complicated by preeclampsia. Reprod Sci. 2008;15(9): 912-920.
[11] Colell A, Ricci JE, Tait S, et al. GAPDH and autophagy preserve survival after apoptotic cytochrome c release in the absence of caspase activation. Cell. 2007;129(5): 983-997.
[12] Gozuacik D, Kimchi A. Autophagy and cell death. Curr Top Dev Biol. 2007;78:217-245.
[13] Maiuri MC, Zalckvar E, Kimchi A, et al. Self-eating and self-killing: crosstalk between autophagy and apoptosis. Nat Rev Mol Cell Biol. 2007;8(9):741-752.
[14] Vinores SA, Herman MM, Rubinstein LJ, et al. Electron microscopic localization of neuron-specific enolase in rat and mouse brain. J Histochem Cytochem. 1984;32(12): 1295-1302.
[15] Oh SY, Choi SJ, Kim KH, et al. Autophagy-related proteins, LC3 and Beclin-1, in placentas from pregnancies complicated by preeclampsia. Reprod Sci. 2008;15(9): 912-920.
[16] Zhang LQ, Niu Q. Mechanism of Cell Apoptosis. Huanjing yu Zhiye Yixue. 2007;24(1):102-107.
[17] Espert L, Denizot M, Grimaldi M, et al. Autophagy is involved in T cell death after binding of HIV-1 envelope proteins to CXCR4. J Clin Invest. 2006;116(8):2161-2172.
[18] Djavaheri-Mergny M, Amelotti M, Mathieu J, et al. NF-kappaB activation represses tumor necrosis factor-alpha-induced autophagy. J Biol Chem. 2006; 281(41):30373-30382.
[19] Zhivotovsky B. Caspases: the enzymes of death. Essays Biochem. 2003;39:25-40.
[20] Philchenkov AA. Caspases as regulators of apoptosis and other cell functions. Biochemistry (Mosc). 2003;68(4): 365-376.
[21] Gavrieli Y, Sherman Y, Ben-Sasson SA. Identification of programmed cell death in situ via specific labeling of nuclear DNA fragmentation. J Cell Biol. 1992;119(3): 493-501.
[22] Liu WL, Zhang Y. Apoptosis detection methods-TUNEL. Jiepou Kexue Jinzhan. 1999;5(4):330-332.
[23] Yen WL, Klionsky DJ. How to live long and prosper: autophagy, mitochondria, and aging. Physiology (Bethesda). 2008;23:248-262.
[24] Herman-Antosiewicz A, Johnson DE, Singh SV. Sulforaphane causes autophagy to inhibit release of cytochrome C and apoptosis in human prostate cancer cells. Cancer Res. 2006;66(11):5828-5835.
[25] Sasnauskiene A, Kadziauskas J, Vezelyte N, et al. Damage targeted to the mitochondrial interior induces autophagy, cell cycle arrest and, only at high doses, apoptosis. Autophagy. 2009;5(5):743-744.
[26] Patschan S, Goligorsky MS. Autophagy: The missing link between non-enzymatically glycated proteins inducing apoptosis and premature senescence of endothelial cells? Autophagy. 2008;4(4):521-523.
[27] State Council of the People's Republic of China. Administrative Regulations on Medical Institution. 1994-09-01.
[28] Casteilla L, Planat-Benard V, Laharrague P, et al. Adipose-derived stromal cells: their identity and uses in clinical trials, an update. World J Stem Cells. 2011;3(4): 25-33.
[29] Maumus M, Peyrafitte JA, D'Angelo R, et al. Native human adipose stromal cells: localization, morphology and phenotype. Int J Obes (Lond). 2011;35(9):1141-1153.
[30] Huang T, He D, Kleiner G, et al. Neuron-like differentiation of adipose-derived stem cells from infant piglets in vitro. J Spinal Cord Med. 2007;30 Suppl 1:S35-40.
[31] Zhou XY, Deng YW, Fang F, et al. Autologous adipose tissue-derived stem cell transplantation for treatment of rats with brain cold injury. Zhongguo Zuzhi Gongcheng Yanjiu yu Linchuang Kangfu. 2008;12(16):3024-3028.
[32] Liu B, Wu MH, Dong J, et al. Neuronal differentiation of adipose tissue-derived stromal cells. Zhongguo Zuzhi Gongcheng Yanjiu yu Linchuang Kangfu. 2010;14(1): 15-18.

(Edited by Bao JF, Yang XF/Qiu Y/Song LP))